Advanced Journal of Chemistry, Section A, 2025, 8(2), 443-455

Advanced Journal of Chemistry, Section A

journal homepage: www.ajchem-a.com

Original Research Article

New Route Producing Large-Scale Graphene Nanosheets from Corn Waste for Electrochemical Material

Kerista Tarigan [1,2] *, Rikson Siburian [2,3] *, Liang Wei Tang [4], Fajar Hutagalung [5], Lewita Pasaribu [2], Yosia Gopas Oetama Manik [3], Ronn Goei [6], Fathan Bahfie [7], Boon Tong Goh [8], Maykel T. E. Manawan [9], Frikson Jony Purba [10]

[1] *Department of Physics, Universitas Sumatera Utara, Medan, Indonesia*
[2] *Carbon Research Center, Universitas Sumatera Utara, Medan, Indonesia*
[3] *Department of Chemistry, Universitas Sumatera Utara, Medan, Indonesia*
[4] *Department of Chemistry, Universiti Malaya, Kuala Lumpur, Malaysia*
[5] *Department of Chemistry, Universitas Sam Ratulangi, Manado, Indonesia*
[6] *Nanyang Environment and Water Research Institute, 1 Cleantech Loop, CleanTech One, Singapore, Republic of Singapore*
[7] *Research Unit for Mineral Technology, Indonesian Institute of Sciences, South Lampung, Indonesia*
[8] *Low Dimensional Materials Research Centre, Department of Physics, Universiti Malaya, Kuala Lumpur, Malaysia*
[9] *National Research and Innovation Agency (BRIN), Tangerang, Banten, Indonesia*
[10] *Department of Elementary School Teacher Education, Universitas Quality, Medan, Indonesia*

ARTICLEINFO

Article history

Submitted: 06 July 2024
Revised: 21 August 2024
Accepted: 12 September 2024
ID: AJCA-2407-1586

DOI: **10.48309/AJCA.2025.466487.1586**

KEYWORDS

Graphene nanosheets
Corn waste
Electrochemical material
Synthesis
Elecrochemical properties

ABSTRACT

In this study, a novel method for synthesizing carbon-containing graphene nanosheets (CCG) from corn cob (CC) waste was developed. The CCG was produced through a two-stage pyrolysis process at various temperatures (200 °C and 300 °C) and durations (0.5, 1, and 1.5 hours). This new method is expected to enhance the graphene quality and offer a cost-effective solution for graphene synthesis from waste materials. The structural characteristics of the CCG were confirmed by X-ray diffraction (XRD), which revealed peaks indicative of graphene, and Fourier transform infrared (FTIR) spectroscopy, which exhibited similarities to previously reported graphene spectra. The optimal CCG sample, synthesized at 300 °C for 0.5 hours followed by 1.5 hours, was characterized by a hexagonal honeycomb structure and achieved the highest carbon content at 87.65% (w/w), as determined by scanning electron microscopy-energy dispersive spectroscopy (SEM-EDS). The electrochemical properties of the CCG were evaluated using cyclic voltammetry (CV), electrochemical impedance spectroscopy (EIS), and linear sweep voltammetry (LSV). Although the charge transfer resistance (R_{ct}) of the CCG-modified glassy carbon electrode (GCE) was found to be higher (3.93 kΩ) compared to the bare GCE (0.30 kΩ), the suboptimal electrochemical performance may be attributed to the presence of impurities, particularly oxygen. Nonetheless, this research highlights the potential of CC waste as a sustainable precursor for the large-scale production of graphene, contributing to the development of eco-friendly materials.

* Corresponding authors: Tarigan, Kerista; Siburian, Rikson
✉ E-mail: kerista@usu.ac.id; rikson@usu.ac.id

GRAPHICAL ABSTRACT

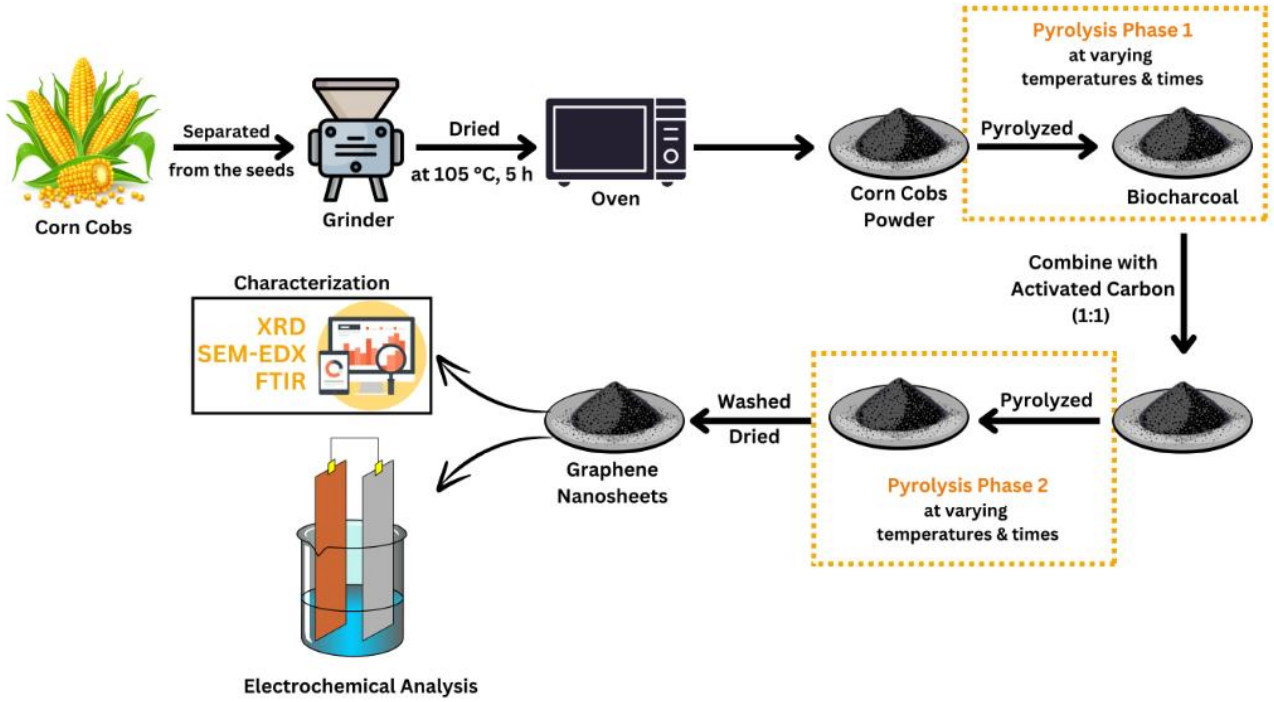

Introduction

In recent years, two-dimensional (2D) graphene, a parent material of graphitic carbon, has become a prominent focus in materials science. Its widespread utilization in diverse energy storage applications (such as batteries, supercapacitors, and fuel cells), sensors, e-textiles, and drug delivery systems emphasized its significance [1-4]. This heightened interest is primarily attributed to graphene's exceptional properties, including its remarkable toughness, lightweight nature, and elastic tensile strength exceeding 130 gigapascals (GPa). Interestingly, previous research has shown that graphene nanosheets (GNS) exhibit exceptional properties not observed in other carbon-supporting materials such as activated carbon (AC), carbon black (CB), carbon nanotubes (CNT), and graphite. In addition, GNS' Young's modulus is approximately 1 terapascal (TPa), enabling it to absorb substantial energy before fracturing. GNS also surpasses most metals, alloys, diamonds, and carbon nanotubes in strength and stiffness [5]. The two-dimensional sheet-like structure of GNS offers a high surface area that is easily accessible to reactants and exhibits minimal mass transfer resistance, setting it apart from traditional porous materials [6]. Single sheets of sp2-hybridized carbon on graphene provide a high electron mobility capability of 106 S/m and a resistance of 31 Ω/sq, which is 140 times higher than silicon [7], making this material valuable in the marketplace [8]. GNS can be produced using either top-down or bottom-up techniques. The top-down approach uses graphite precursors or other carbon sources like cellulose, glucose, coal, or biomass [9,10]. These precursors undergo structural changes to reduce multilayer carbon to a few layers or a single graphene nanosheet layer. In contrast, the bottom-up method uses precursors such as methane gas, acetylene, and pyridine, where solid carbon molecules bond together to form

hexagonal planar C-C covalent bonds with the help of a catalyst. Graphene can also be synthesized from biomass using various methods, including chemical vapor deposition, thermal pyrolysis, electrochemical oxidation, microwave plasma irradiation, laser-induced carbonization, and emulsion template carbonization [11,12]. Previous work has successfully synthesized graphene from agricultural products like corn flour using the Hummers redox method [13].

Furthermore, other studies have used biomass from waste materials to produce graphene. Various by-products and waste materials are generated from composting [14], lignocellulosic biomass, biodiesel [15], biogas, biohydrogen [13], and methane production. Processing and recycling these wastes, especially those from agro-industrial sources like fruit, vegetable, and plant residues, is becoming increasingly important.

Agricultural waste poses a critical environmental challenge, with residues generated during the production and processing of raw agricultural goods. The escalating concerns regarding climate change and natural water resource depletion necessitate innovative approaches to address these challenges, fostering a circular economy through efficient agricultural waste recycling [16].

In recent years, agricultural wastes have become vital sources of raw materials for graphene synthesis, including pomelo peels using laser method [17], corn husk [18], spent black tea bags [19], subabul, pine, and copper pod biomass waste [20]. Corn cobs (CC) constitute a substantial portion of these agricultural wastes. Projections indicate a steady rise in global corn production, with an estimated annual output of 1143 million tons by 2025. Leading corn-producing nations include the USA, China, Brazil, Argentina, India, and Indonesia [21].

CC has been utilized as bioethanol, composite board, and animal feed, but it also has an enormous potential as a graphene precursor. CC has reasonably high cellulose content with 37.8 ± 1.56% cellulose, 42.2 ± 1.68% hemicellulose, and 12.7 ± 1.23% lignin [22]. The cellulose content can be isolated as a precursor for graphene synthesis using the activation-pyrolysis method at 700, 800, and 900 °C [23]. Previous research has successfully produced activated carbon from CC using the pyrolysis method at 1000 °C under argon gas. The product has revealed visible Raman data on 2D bands with weak and broad peaks, indicating graphene formation [24]. This method is favored for its simplicity and lack of harmful chemicals, making it an environmentally friendly approach (green synthesis).

Graphene derived from biomass can be produced by pyrolysis, as reported in a previous study, by converting coconut into graphite and graphene using the heat reduction method using AC [25]. This method is considered as a cost-effective and simple method to synthesize graphene, which supports the fabrication of graphene and N-graphene on a large scale [26]. The carbon-containing GNS (CCG) results are confirmed with the conditions of the ID/IG ratio of 0.85, known as a multilayer with a distance of 0.33 nm between graphene layers [27].

However, large-scale production of GNS remains challenging [28]. Therefore, this study aims to explore large-scale production of GNS using renewable raw materials, specifically CC waste. The novelty of this study lies in the innovative approach of synthesizing graphene from CC waste using pyrolysis and reduction methods at relatively low temperatures. This method is advantageous because it reduces the energy requirements typically associated with graphene production and leverages biomass precursors, which are both affordable and widely accessible. In addition, biomass supports sustainability, making this approach a promising pathway for developing eco-friendly and cost-effective solutions in clean energy technologies [26].

Materials and Methods

Materials and instrumentations

The materials used include CC feedstocks obtained from agro-industrial waste in North Sumatra, Indonesia, AC (E-Merck) as a reductant, and distilled water to produce CCG. Furthermore, consumables like Al foil and mesh were also used. The synthesized materials underwent characterization using scanning electron microscope-energy dispersive spectroscopy (SEM-EDS; JEOL JSM-5310), X-ray diffraction (XRD; Rigaku Corporation), and Fourier transform infrared (FTIR; Perkin Elmer 100). Electrochemical assessments were also conducted for CC without treatment or bare CC, and the obtained CCG using a Potentiostat/Galvanostat (Autolab PGSTAT30, Eco-chemie Netherlands), glassy carbon working electrode (GCE) with a diameter of 3 mm (Sigma-Aldrich), platinum rod counter electrode (HY Electronic), Ag/AgCl reference electrode (Thermo Scientific), and ultrasonication homogenizer (UH-650, B-One). Chemicals including KCl, $[Fe(CN)_6]^{3-/4-}$, and KOH (all obtained from E-Merck) were used in the sample preparation for electrochemical measurements. This study used the pyrolysis method to produce graphene, which has been successfully conducted by Supeno and Siburian [25], but instead of using coconut shells, this research used CC. Furthermore, this study intends to use a more green approach by employing a lower pyrolysis temperature (200 and 300 °C) than the previous work (600 °C) and minimal chemicals.

Biocharcoal production

The CC was separated from the seeds and ground into smaller sizes using a grinder., and then the CC was dried in the sun. The dried CC was further dried in an oven at 105 °C for 5 h to eliminate the excess water.

Afterwards, the completely dried CC was conventionally pyrolyzed at 200 °C for 1 h to form charcoal. Pyrolysis was selected for its significant benefits, including simplicity and efficiency. This method converts carbon-containing waste into graphene through thermal decomposition in the absence of oxygen, resulting in high-quality graphene with well-controlled particle size and distribution. In addition, pyrolysis can be performed at relatively lower temperatures than other methods, such as chemical vapor deposition (CVD), reducing operational and energy costs.

CCG production

The ash attached to the charcoal produced from the CC was removed using a brush. Afterward, the charcoal was combined with AC powder in a 1:1 ratio and then subjected to another round of pyrolysis at 200 °C for 1 h. The second phase of pyrolysis aims to enhance the quality of the graphene produced further. Expected results from this phase include improved crystallinity, better structural ordering, increased electrical conductivity, and reduced structural defects. The resulting chip-shaped CCG was rinsed with distilled water and dried in an oven at 105 °C for 2 h. The same experiment was carried out on producing bio charcoal and CCG with variations of temperature ($T_{Pyrolysis}$; °C): time ($t_{Pyrolysis}$-1; h): time ($t_{Pyrolysis}$-2; h) of 300: 0.5: 1; 300: 0.5: 1.5; 200: 1: 1.5; 200:1.5: 1; 200: 1.5: 1.5.

Characterization

The CCG and untreated CC underwent analysis using XRD, SEM-EDX, and FTIR to confirm the successful synthesis of CCG. XRD was used to assess structural and compositional properties. SEM-EDX was employed to study the morphological surface of CCG. Meanwhile, FTIR was used to evaluate the functional groups in the CCG structure.

Table 1. Corn CCG yields

Variations	Mass		CCG Yields (%w/w)
	Before Treatment	After Treatment	
300 °C; 0.5 h; 1h	50 g	7.8 g	15.6
300 °C; 0.5 h; 1.5 h	50 g	8.0 g	16.0
200 °C; 1 h; 1 h	50 g	7.9 g	15.8
200 °C; 1 h; 1.5 h	50 g	7.6 g	15.2
200 °C; 1.5 h; 1 h	50 g	7.7 g	15.4
200 °C; 1.5 h; 1.5 h	50 g	8.2 g	16.4

Electrochemical analysis

The electrochemical setup consisted of a modified GCE with a diameter of 3 mm, an Ag/AgCl reference electrode, and a platinum rod counter electrode. Before use, the GCE underwent polishing with Al powder and thorough rinsing with distilled water. A homogenized suspension of CCG at a concentration of 1 mg/mL was set by dispersing the synthesized CCG in distilled water using ultrasonication for 0.5 hours. Following this, 5 µL of the suspension was drop-casted onto the surface of the GCE and allowed to air-dry at room temperature, forming CCG/GCE.

The prepared electrode underwent analysis utilizing cyclic voltammetry (CV), electrochemical impedance spectroscopy (EIS), and linear sweep voltammetry (LSV) within a three-electrode system to assess the electrical properties of CCG and explore its potential applications. CV analysis of GCE and CCG/GCE was conducted in 1 M KOH at a scan rate of 50 mV/s. EIS assessments were conducted with an AC amplitude of 5 mV, utilizing frequency sweeps ranging from 10 kHz to 0.1 Hz in 0.1 M KCl with 5 mM $[Fe(CN)_6]^{3-/4-}$. Meanwhile, the oxygen evolution reaction (OER) of the CCG/GCE was investigated using LSV by scanning from 0 to 2 V in 1 M KOH at 20 mV/s.

Results and Discussion

CCG yields

Based on the results of the CC pyrolysis, the % yield of CCG for each variation of temperature ($T_{Pyrolysis}$) and time ($t_{Pyrolysis}$-1 and $t_{Pyrolysis}$-2) was determined using Equation (1), and the results are summarized in Table 1.

$$\%\text{Yield of CCG} = (\text{Weight CCG})/(\text{Weight CC}) \times 100\% \quad (1)$$

According to Table 1, the mass of all CC converted to CCG decreased substantially, approximately 85% of the total weight after heat treatment. This reduction corresponds to releasing O_2, CO_2, and H_2O molecules from heat treatment.

XRD analysis

XRD analysis utilized a beam size of 10 mm × 10 mm, employing monochromator Cu/Kα radiation (α = 1.5406) at 40 kV and 100 mA. The scanning range spanned from 10 to 80° (2θ) with 2.0° increments. Powder XRD patterns were acquired using a SWXD diffractometer working at 18 kW, generating a 2D diffraction pattern from the sample.

The XRD image depicted a notable impact of variation on crystallinity behavior (Figure 1). In the six variations of CCG samples, the C (002) peak exhibited a broad and weak pattern, suggesting a tendency towards amorphous crystallinity, consistent with JCPDS Card 008-0416.

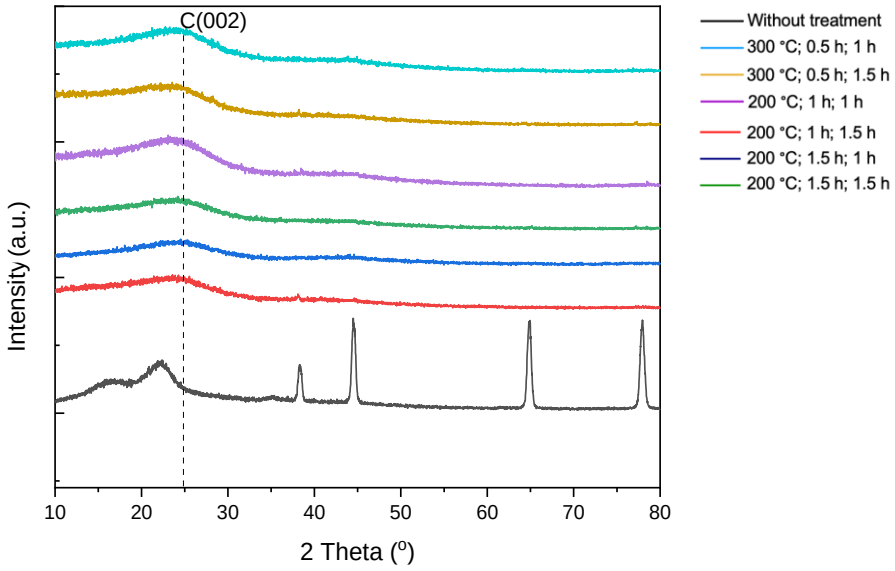

Figure 1. XRD diffractogram of CCG and CC samples.

Liu *et al.* [29] proved that the nano-sized graphene layer stacked C (002) diffraction pattern has a peak at 2θ = 24–26° with a weak broad peak. Analysis of the diffractogram revealed that all variations of CCG displayed a C (002) peak at 2θ = 24.3°, consistent with the literature. Meanwhile, the cellulose crystallinity peak was evident in the untreated CC diffraction pattern, manifesting as weak and broadened peaks at 2θ = 16.7° and 21.9°, indicating that the cellulose was amorphous. This finding was in accordance with the reported work that found the cellulose demonstrating amorphous peaks at 2θ = 16.7°, 21.9°, and 28.2° [30]. Furthermore, lignin nanofibers exhibited peaks at 2θ = 38.2°, 44.5°, 64.9°, and 77.9°. Lignin nanofiber was identified in the diffractogram due to the high degradation temperature of lignin, making it still attached to the sample. However, 300 °C; 0.5 h; 1.5 h variation indicated a weak lignin peak resembling the graphene diffractogram.

Morphological properties of corn CCG

The obtained CCG underwent SEM-EDS characterization to examine its surface morphology at a magnification of 20,000 times. As depicted in Figure 2, each variation can be interpreted based on distinct morphologies.

Figure 2a reveals that the CC without treatment exhibited hole-like structures with irregular shapes. Meanwhile, the sample with a temperature variation of 300 °C has loosely arranged C-C structures detached from other carbon structures, initiating the formation of pores (Figure 2b). Furthermore, longer heating times at 300 °C led to improved results. It displayed larger pores, displaying a tighter hexagonal honeycomb graphene structure, representing an optimal surface morphology (Figure 2c). The pores in the material might indicate the presence of voids or spaces within the structure, making it a three-dimensional porous graphene nanosheet [31]. These could be due to various factors, such as the evaporation of gases during pyrolysis, the removal of functional groups, or even the structural rearrangement of carbon atoms. In contrast, the structure at a temperature variation of 200 °C in Figure 2d showed minimal change compared to untreated CC. Figure 2e exhibits a variation with structural defects, where the specific type of structure could not be determined. However, the formation of graphene layers was observed.

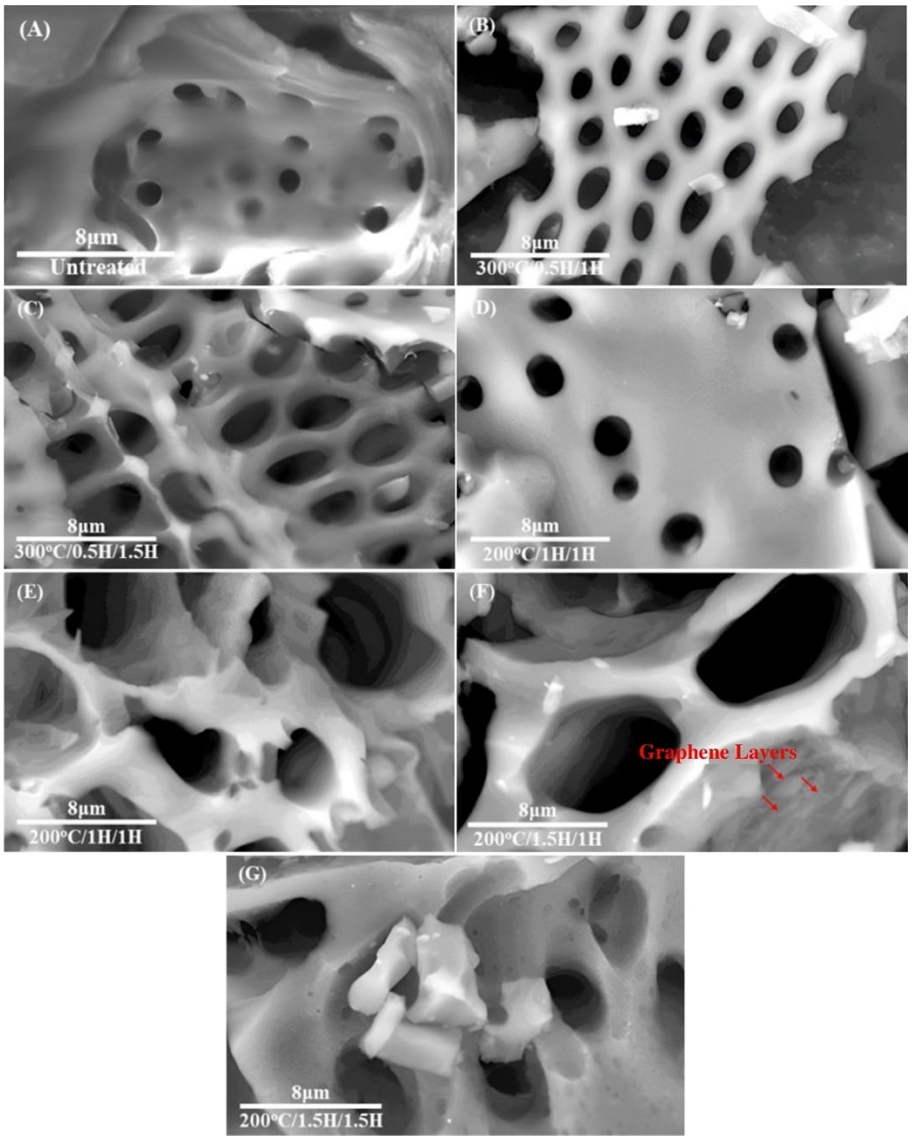

Figure 2. SEM images of (a) CC without treatment and CCG synthesized at (b) 300 °C; 0.5 h; 1 h, (c) 300 °C; 0.5 h; 1.5 h, (d) 200 °C; 1 h; 1 h, (e) 200 °C; 1 h; 1.5 h, (f) 200 °C; 1.5 h; 1 h, and (g) 200 °C; 1.5 h; 1.5 h.

In addition, Figure 2f displays a variation where the structure had begun to form but had not fully developed into a hexagonal shape, with a noticeable enlargement of pores.

Meanwhile, the variation depicted in Figure 2g lacked conclusive structures, with only pores showing enlargement as temperature and duration increased. According to the EDX data in Table 2, the carbon content in the samples varied significantly. The untreated corn sample showed a carbon concentration of 73.00%, whereas the most optimal variation, 300 °C; 0.5 h; 1.5 h, achieved a notably higher carbon concentration of 87.65%. This variation also yielded the best morphological structure, likely due to more complete oxygen reduction, facilitated by prolonged contact time of the AC reductant with the sample, promoting oxygen termination reactions. However, variations treated at 200 °C exhibited high carbon content but failed to acquire hexagonal morphology, possibly due to increased carbon content caused by water evaporation.

Table 2. EDS data of CCG with different variations

Variations	Atomic Concentration (%)		Weight Concentration (%)	
	C	O	C	O
Without treatment	73.00	27.00	67.0	33.0
300 °C; 0.5 h; 1 h	84.78	15.22	80.7	19.3
300 °C; 0.5 h; 1.5 h	87.65	12.35	84.2	15.8
200 °C; 1 h; 1 h	86.26	13.74	82.5	17.5
200 °C; 1 h; 1.5 h	79.90	20.10	74.9	25.1
200 °C; 1.5 h; 1 h	81.35	18.65	76.6	23.4
200 °C; 1.5 h; 1.5 h	87.97	12.03	84.6	15.4

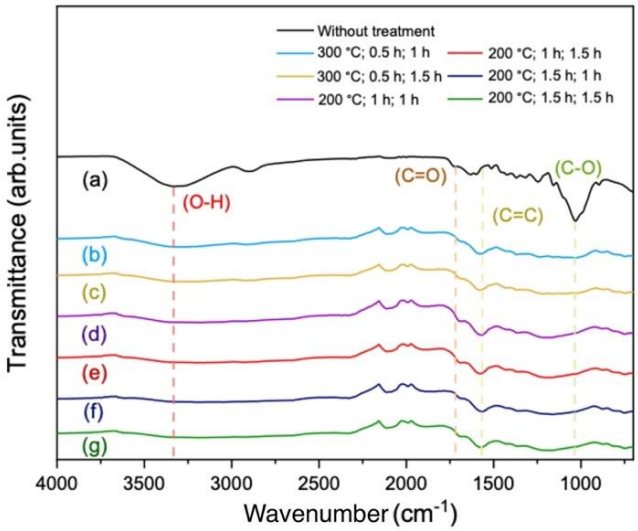

Figure 3. FTIR spectrum of (a) CC without treatment and CCG synthesized at (b) 300 °C; 0.5 h; 1 h, (c) 300 °C; 0.5 h; 1.5 h, (d) 200 °C; 1 h; 1 h, (e) 200 °C; 1 h; 1.5 h, (f) 200 °C; 1.5 h; 1 h, and (g) 200 °C; 1.5 h; 1.5.

FTIR characterization

FTIR characterization was done to identify the functional groups of the CCG materials. Figure 3 showed the FTIR spectra of CCG and untreated CC. FTIR spectrum of untreated CC demonstrated a strong and broad O-H stretching vibration band at 3332 cm^{-1}, carboxyl CHO stretching band at 1632 cm^{-1}, and C-O stretching vibration at 1087 cm^{-1} [32]. The results were in accordance with the literature, which indicated that the wavenumber of the C=C–C aromatic ring stretch was identified at 1615–1580 and 1510–1450 cm^{-1}, and –OH stretching at 3332 cm^{-1} [33]. Due to the reduction reaction by AC, these peaks were relatively diminished or entirely absent in the FTIR spectra of CCG, similar to the graphene FTIR spectrum reported elsewhere [34]. These results indicated that CCG was successfully obtained after the reduction reaction.

Electrochemical measurements of Corn CCG

The electrochemical characteristics of CCG were assessed using CCG/GCE (glassy carbon working electrode). As illustrated in Figure 4a, the CV curves depict the redox behavior of the fabricated electrodes in 0.1 M KCl with 5 mM $[Fe(CN)_6]^{3-/4-}$. A lower current response was observed for CCG/GCE compared to bare GCE. Figure 4b illustrates the EIS results based on Nyquist plots where the charge transfer

resistance (R_{ct}) of bare GCE and CCG/GCE acquired were 0.30 kΩ and 3.93 kΩ, respectively. The CV and EIS results were in good agreement.

Furthermore, the specific capacitance of bare GCE (50.4 F/g) and CCG/GCE (26.9 F/g) was determined by analyzing CV curves recorded in 1 M KOH at 50 mV/s (Figure 4c). Figure 4d further demonstrates the OER using LSV, where the response obtained from CCG/GCE was poorer than that from bare GCE. These findings hold significance in elucidating the possible applications of these materials in energy storage and electrochemical devices. Doping of CCG with metals or halogens is recommended to enhance the electrical properties due to their potential to improve electrical conductivity.

According to the CV plots (Figure 4c) and LSV plots (Figure 4d), the CCG data compared to bare GCE indicate suboptimal values. However, the increase in charge transfer resistance (R_{ct}) after synthesizing graphene suggests that the modification may have created a barrier to electron flow, likely due to the carbon material's porosity, surface area, and chemical composition. This is attributed to the significant amount of impurities, particularly oxygen, leading to increased current resistance, thus rendering bare GCE more conductive [35].

This challenge can be addressed by increasing the reduction temperature and the mass of the reducing agent.

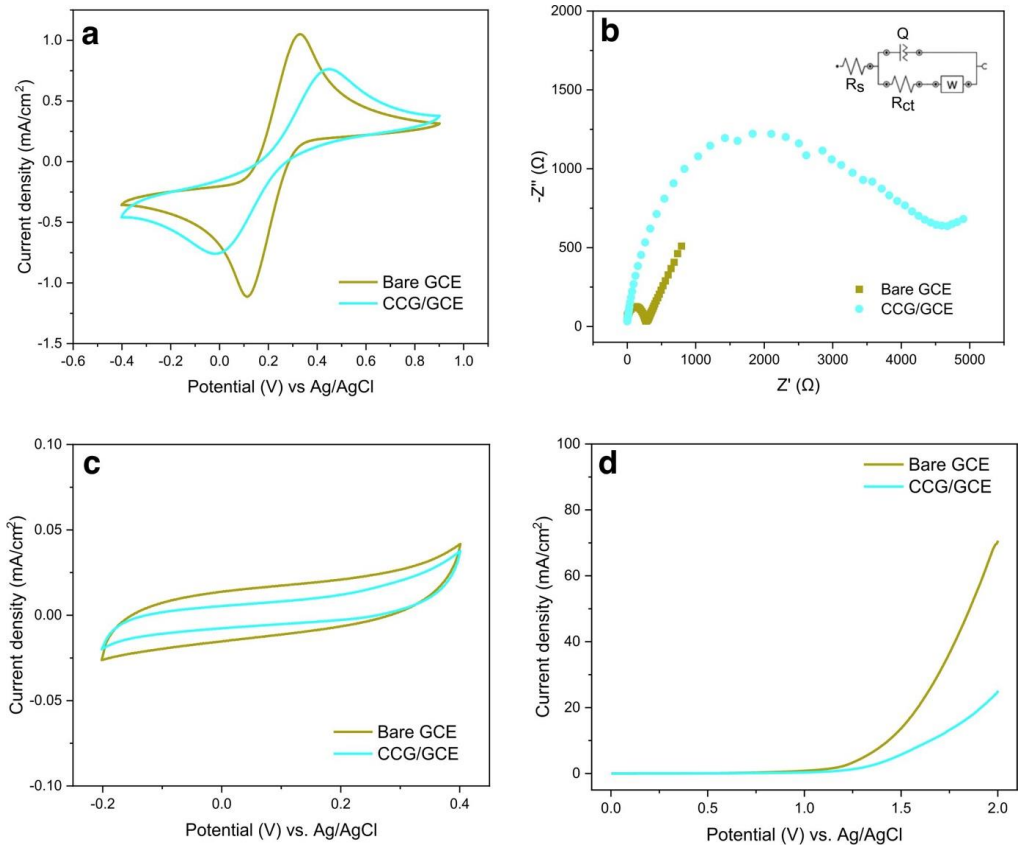

Figure 4. (a) CV curves of bare GCE and CCG/GCE recorded in 0.1 M KCl solution with 5 mM $[Fe(CN)_6]^{3-/4-}$ at a scan rate of 50 mV/s, (b) Nyquist plots of bare GCE and CCG/GCE recorded in 0.1 M KCl solution with 5 mM $[Fe(CN)_6]^{3-/4-}$; inset is the equivalent electrical circuit model, (c) CV curves of bare GCE and CCG/GCE recorded in 1 M KOH at a scan rate of 50 mV/s, and (d) LSV of bare GCE and CCG/GCE recorded in 1 M KOH at a scan rate of 20 mV/s.

Table 3. Comparison with other works

Synthesis Method	Compared Variable (R_{ct})	Ref.
Two-stage pyrolysis from corn waste	Bare GCE 0.30 kΩ Graphene/GCE 3.93 kΩ	This work
One-stage pyrolysis from coconut waste	Bare GCE 0.30 kΩ Graphene/GCE 0.88 kΩ	[36]
Hydrothermal method	Bare GCE 0.20 kΩ MoS_2 NSAs/rGO/GCE 0.11 kΩ	[37]
Hummer method	Bare GCE 2.63 kΩ NiO/CoO@PCNs/CNTs/erGO/GCE 0.22 kΩ	[38]

Compared to another synthesis method, the two-stage pyrolysis used in this article gives similar results with coconut-driven CCG, which is also a biomass-based CCG but in contrast with other CCG, as seen in Table 3. Based on Table 3, it can be concluded that biomass-driven CCG will give similar R_{ct} results compared to conventional precursor-driven CCG. The biomass-driven CCG has the advantage of a more efficient and environmentally friendly synthesis method.

Conclusion

To sum up, the optimal conditions for synthesizing CCG were achieved with a pyrolysis temperature ($T_{Pyrolysis}$) of 300 °C and pyrolysis durations ($t_{Pyrolysis}$-1 and -2) of 0.5 and 1.5 h, respectively. This specific variation yielded a carbon content of 87.65% and exhibited honeycomb morphology akin to hexagonal planar structures. The study revealed the effect of pyrolysis temperature and duration on the morphological characteristics of CCG. The AC application as a reductant for oxide groups was confirmed through FTIR analysis, revealing the absence of a peak at 3332 cm^{-1} for hydroxyl groups. These observations indicated the successful conversion of cellulose into CCG. The successful synthesis of CCG from CC was further confirmed through XRD and SEM-EDS characterizations. However, despite successful synthesis, the electrochemical performance of the obtained CCG was unsatisfactory, as evidenced by CV, EIS, and LSV results. This poor electrochemical response highlights the need for further research to enhance its performance. Future research could explore doping techniques and the development of CCG nanocomposites to improve their electrochemical properties.

Acknowledgements

The authors are grateful to PT Dynatech International for conducting the SEM-EDS analysis. In addition, the authors would like to thank the Rector of Universitas Sumatera Utara for the financial support provided for this study, with Reference Number: 24/UN5.2.3.1/PPM/KP-TALENTA/R/2023.

Disclosure statement

No potential conflict of interest was reported by the authors.

Orcid

Kerista Tarigan: 0000-0001-8597-6544
Rikson Siburian: 0000-0001-7836-0389
Liang Wei Tang: 0000-0002-6895-237X
Fajar Hutagalung: 0009-0004-4013-0958
Lewita Pasaribu: 0009-0007-2605-0283
Yosia Gopas Oetama Manik: 0000-0002-6305-4327
Ronn Goei: 0000-0001-6794-0601
Fathan Bahfie: 0000-0003-3460-469X

Boon Tong Goh: https://orcid.org/0000-0003-3933-7594
Maykel T. E. Manawan: 0000-0003-3782-1307
Frikson Jony Purba: 0000-0002-8504-4293

References

[1] R. Siburian, F. Hutagalung, O. Silitonga, S. Paiman, L. Simatupang, C. Simanjuntak, S.P. Aritonang, Y. Alias, L. Jing, R. Goei, The new materials for battery electrode prototypes, *Materials*, **2023**, *16*, 555. [Crossref], [Google Scholar], [Publisher]

[2] J. Liu, S. Bao, X. Wang, Applications of graphene-based materials in sensors: A review, *Micromachines*, **2022**, *13*, 184. [Crossref], [Google Scholar], [Publisher]

[3] M.R. Islam, S. Afroj, C. Beach, M.H. Islam, C. Parraman, A. Abdelkader, A.J. Casson, K.S. Novoselov, N. Karim, Fully printed and multifunctional graphene-based wearable e-textiles for personalized healthcare applications, *IScience*, **2022**, *25*. [Google Scholar], [Publisher]

[4] B. Liu, W. Yang, C. Che, J. Liu, M. Si, Z. Gong, R. Gao, G. Yang, A targeted nano drug delivery system of AS1411 functionalized graphene oxide-based composites, *ChemistryOpen*, **2021**, *10*, 408-413. [Crossref], [Google Scholar], [Publisher]

[5] Y. Sun, D. Papageorgiou, C. Humphreys, D. Dunstan, P. Puech, J. Proctor, C. Bousige, D. Machon, A. San-Miguel, Mechanical properties of graphene, *Applied Physics Reviews*, **2021**, *8*. [Crossref], [Google Scholar], [Publisher]

[6] A. Khazaee, R. Jahanshahi, S. Sobhani, J. Skibsted, J.M. Sansano, Immobilized piperazine on the surface of graphene oxide as a heterogeneous bifunctional acid–base catalyst for the multicomponent synthesis of 2-amino-3-cyano-4 H-chromenes, *Green Chemistry*, **2020**, *22*, 4604-4616. [Crossref], [Google Scholar], [Publisher]

[7] V.B. Mbayachi, E. Ndayiragije, T. Sammani, S. Taj, E.R. Mbuta, Graphene synthesis, characterization and its applications: A review, *Results in Chemistry*, **2021**, *3*, 100163. [Crossref], [Google Scholar], [Publisher]

[8] Y. Zhu, H. Ji, H.-M. Cheng, R.S. Ruoff, Mass production and industrial applications of graphene materials, *National Science Review*, **2018**, *5*, 90-101. [Crossref], [Google Scholar], [Publisher]

[9] S. Liu, J. Xue, X. Liu, H. Chen, X. Li, Pitch derived graphene oxides: Characterization and effect on pyrolysis and carbonization of coal tar pitch, *Journal of Analytical and Applied Pyrolysis*, **2020**, *145*, 104746. [Crossref], [Google Scholar], [Publisher]

[10] M. Chen, J. Li, J. Zhang, Y. Ma, H. Dong, W. Li, E. Bekyarova, Y.F. Al-Hadeethi, L. Chen, M.N. Hedhili, Evolution of cellulose acetate to monolayer graphene, *Carbon*, **2021**, *174*, 24-35. [Crossref], [Google Scholar], [Publisher]

[11] J.K. Saha, A. Dutta, A review of graphene: material synthesis from biomass sources, *Waste and Biomass Valorization*, **2022**, 1-45. [Crossref], [Google Scholar], [Publisher]

[12] X. Zhang, X. Ma, Z. Yu, Y. Yi, C. Lu, X. Lu, Microwave-assisted two-step pyrolysis of water hyacinth for the preparation of N-self-doped porous carbon, *Journal of Analytical and Applied Pyrolysis*, **2023**, *173*, 106061. [Crossref], [Google Scholar], [Publisher]

[13] A.J.F.T. Balbin, H.A. Gonzales, L.A.M. Bornillo, J.H.A. Tagupa, R.H. Jaro, A.L. Ido, R.O. Arazo, High biohydrogen yield from fresh cassava waste pulps via gas dissolution in a dark fermentative environment, *Cleaner Waste Systems*, **2022**, *3*, 100039. [Crossref], [Google Scholar], [Publisher]

[14] N. Leeabai, C. Siripaiboon, K. Taweengern, C. Buttanoo, W. Sujirapatpong, D. Yimyam, F. Takahashi, C. Areeprasert, The integrated study of the effects of infographic design on waste separation behavior and the behavioral outcome implementation on waste

composting, *Waste Management*, **2023**, *169*, 276-285. [Crossref], [Google Scholar], [Publisher]

[15] W.M. Kedir, K.T. Wondimu, G.S. Weldegrum, Optimization and characterization of biodiesel from waste cooking oil using modified CaO catalyst derived from snail shell, *Heliyon*, **2023**, *9*. [Google Scholar], [Publisher]

[16] P. Wu, S. Li, Does the risk of oil and energy based resources extraction Hinder or Foster sustainable development?, *Resources Policy*, **2023**, *85*, 104004. [Crossref], [Google Scholar], [Publisher]

[17] S. Liu, J. Xue, X. Liu, H. Chen, X. Li, Pitch derived graphene oxides: Characterization and effect on pyrolysis and carbonization of coal tar pitch, *Journal of Analytical and Applied Pyrolysis*, **2020**, *145*, 104746. [Crossref], [Google Scholar], [Publisher]

[18] C. Chailuecha, A. Klinbumrung, P. Chaopanich, R. Sirirak, Graphene-like porous carbon nanostructure from corn husk: synthesis and characterization, *Materials Today: Proceedings*, **2021**, *47*, 3525-3528. [Crossref], [Google Scholar], [Publisher]

[19] A. Abbas, S. Rubab, A. Rehman, S. Irfan, H. Sharif, Q. Liang, T. Tabish, One-step green synthesis of biomass-derived graphene quantum dots as a highly selective optical sensing probe, *Materials Today Chemistry*, **2023**, *30*, 101555. [Crossref], [Google Scholar], [Publisher]

[20] R. Mishra, A. Kumar, E. Singh, A. Kumari, S. Kumar, Synthesis of graphene oxide from biomass waste: Characterization and volatile organic compounds removal, *Process Safety and Environmental Protection*, **2023**, *180*, 800-807. [Crossref], [Google Scholar], [Publisher]

[21] N. Tanklevska, V. Petrenko, A. Karnaushenko, K. Melnykova, World corn market: analysis, trends and prospects of its deep processing, *Agricultural and Resource Economics: International Scientific E-Journal*, **2020**, *6*, 96-111. [Crossref], [Google Scholar], [Publisher]

[22] F.M. Olajuyigbe, C.O. Fatokun, O.I. Oni, Effective Substrate Loading for Saccharification of Corn Cob and Concurrent Production of Lignocellulolytic Enzymes by Fusarium oxysporum and Sporothrix carnis, *Current Biotechnology*, **2019**, *8*, 109-115. [Crossref], [Google Scholar], [Publisher]

[23] D. Perondi, G.R. Bassanesi, C. Manera, L.K. Lazzari, M. Godinho, A.J. Zattera, G.L. Dotto, From cellulose to graphene-like porous carbon nanosheets, *Microporous and Mesoporous Materials*, **2021**, *323*, 111217. [Crossref], [Google Scholar], [Publisher]

[24] S. Ghosh, R. Santhosh, S. Jeniffer, V. Raghavan, G. Jacob, K. Nanaji, P. Kollu, S.K. Jeong, A.N. Grace, Natural biomass derived hard carbon and activated carbons as electrochemical supercapacitor electrodes, *Scientific Reports*, **2019**, *9*, 16315. [Crossref], [Google Scholar], [Publisher]

[25] M. Supeno, R. Siburian, New route: Convertion of coconut shell tobe graphite and graphene nano sheets, *Journal of King Saud University-Science*, **2020**, *32*, 189-190. [Crossref], [Google Scholar], [Publisher]

[26] R. Siburian, L.W. Tang, Y. Alias, A.I.Y. Tok, R. Goei, C. Simanjuntak, K. Tarigan, S. Paiman, B.T. Goh, I. Anshori, Coconut waste to green nanomaterial: Large scale synthesis of *N*-doped graphene nano sheets, *Nano-Structures & Nano-Objects*, **2023**, *36*, 101061. [Crossref], [Google Scholar], [Publisher]

[27] E. Pasaribu, R. Siburian, M. Supeno, Production of graphene by coconut shell as an electrode primary battery cell, *Elkawnie: Journal of Islamic Science and Technology*, **2023**, *9*, 37-47. [Crossref], [Google Scholar], [Publisher]

[28] R. Siburian, H. Sihotang, S.L. Raja, M. Supeno, C. Simanjuntak, New route to synthesize of graphene nano sheets, *Oriental Journal of*

Chemistry, **2018**, *34*, 182. [Crossref], [Google Scholar], [Publisher]

[29] X. Liu, C.Z. Wang, M. Hupalo, H.Q. Lin, K.M. Ho, M.C. Tringides, Metals on graphene: interactions, growth morphology, and thermal stability, *Crystals*, **2013**, *3*, 79-111. [Crossref], [Google Scholar], [Publisher]

[30] Q. Yu, X. Kong, Y. Ma, R. Wang, Q. Liu, J.P. Hinestroza, A.X. Wang, T. Vuorinen, Multi-functional regenerated cellulose fibers decorated with plasmonic Au nanoparticles for colorimetry and SERS assays, *Cellulose*, **2018**, *25*, 6041-6053. [Crossref], [Google Scholar], [Publisher]

[31] J. Qiu, J. Guo, H. Geng, W. Qian, X. Liu, Three-dimensional porous graphene nanosheets synthesized on the titanium surface for osteogenic differentiation of rat bone mesenchymal stem cells, *Carbon*, **2017**, *125*, 227-235. [Crossref], [Google Scholar], [Publisher]

[32] T.M. Magne, T. de O. Vieira, L.M.R. Alencar, F.F.M. Junior, S. Gemini-Piperni, S.V. Carneiro, L.M. U.D. Fechine, R.M. Freire, K. Golokhvast, P. Metrangolo, P.B.A. Fechine, R. Santos-Oliveira, Graphene and its derivatives: understanding the main chemical and medicinal chemistry roles for biomedical applications, *Journal of Nanostructure in Chemistry*, **2022**, *12*, 693–727. [Crossref], [Google Scholar], [Publisher]

[33] A.B.D. Nandiyanto, R. Oktiani, R. Ragadhita, How to read and interpret FTIR spectroscope of organic material, *Indonesian Journal of Science and Technology*, **2019**, *4*, 97-118. [Google Scholar], [Publisher]

[34] B. Anegbe, I.H. Ifijen, M. Maliki, I.E. Uwidia, A.I. Aigbodion, Graphene oxide synthesis and applications in emerging contaminant removal: a comprehensive review, *Environmental Sciences Europe*, **2024**, *36*, 15. [Crossref], [Google Scholar], [Publisher]

[35] J. Koettgen, M. Martin, The ionic conductivity of Sm-doped ceria, *Journal of the American Ceramic Society*, **2020**, *103*, 3776-3787. [Crossref], [Google Scholar], [Publisher]

[36] K. Tarigan, R. Siburian, I. Anshorie, N. Widiarti, Y.B. Alias, B.T. Goh, J. Huang, F. Bahfie, Y.G.O. Manik, R. Goei, Synthesis and characterization of coconut-derived graphene and its properties in nickel/graphene and zinc/graphene electrodes, **2024**, *12*, 1943. [Crossref], [Google Scholar], [Publisher]

[37] R. Nehru, B.S. Kumar, C.W. Chen, C.D. Dong, Sphere-like MoS2 nanosheet arrays/reduced graphene oxide hybrid electrocatalyst for accurate electrochemical monitoring of toxic pollutant, *Journal of Environmental Chemical Engineering*, **2022**, *10*, 108687. [Crossref], [Google Scholar], [Publisher]

[38] L. Zhang, J. Tang, J. Li, Y. Li, P. Yang, P. Zhao, J. Fei, Y. Xie, A novel dopamine electrochemical sensor based on 3D flake nickel oxide/cobalt oxide@ porous carbon nanosheets/carbon nanotubes/electrochemical reduced of graphene oxide composites modified glassy carbon electrode, *Colloids and Surfaces A: Physicochemical and Engineering Aspects*, **2023**, *666*, 131284. [Crossref], [Google Scholar], [Publisher]

HOW TO CITE THIS ARTICLE

K. Tarigan, R. Siburian, L.W. Tang, F. Hutagalung, L. Pasaribu, Y.G. Oetama Manik, R. Goei, F. Bahfie, B.T. Goh, M.T.E. Manawan, F.J. Purba. New Route Producing Large-Scale Graphene Nanosheets from Corn Waste for Electrochemical Material. *Adv. J. Chem. A*, 2025, 8(2), 443-455.

DOI: 10.48309/AJCA.2025.466487.1586
URL: https://www.ajchem-a.com/article_205140.html